

# Torsional Vibration and Static Analysis of the Cylindrical Shell Based on Strain Gradient Theory

Hamid Zeighampour<sup>1</sup> · Yaghoub Tadi Beni<sup>1</sup> · Iman Karimipour<sup>1</sup>

Received: 23 May 2015 / Accepted: 19 October 2015 / Published online: 3 November 2015  
© King Fahd University of Petroleum & Minerals 2015

**Abstract** In this paper, the free vibration and torsional static analysis of cylindrical shell are developed using modified strain gradient theory. In doing this, the governing equations and classical and non-classical boundary conditions are derived using Hamilton's principle. After obtaining equations governing the problem, the differential quadrature method is used to discretize the equations of motion of the vibration problem and to examine the single-walled carbon nanotube (SWCNT) with two clamped-free and clamped-clamped supports as a special application of this formulation. Also, torsional static analysis is carried out for the clamped-clamped SWCNT. Results reveal that SWCNT rigidity in strain gradient theory is higher than that in couple stress theory or the classical theory, which leads to increase in torsional frequencies and decrease in torsion of SWCNT. Results also demonstrate that the effect of size parameter and SWCNT torsion in different lengths and diameters is considerable.

**Keywords** Torsional vibration · Static analysis · Cylindrical shell · Modified strain gradient theory · Size effect

## 1 Introduction

Torsional vibration and static analysis of single-walled carbon nanotubes (SWCNTs) are very significant in designing nano-devices such as nano-sensors, nano-oscillators and nano-actuators under torsion. Besides, examination of

dynamic behavior of such nano-structures demands complete knowledge of their dynamic behavior during torsional vibration. It is impossible, due to the minute size of SWCNTs, to study their dynamic behavior and mechanical properties using traditional methods and hence the use of methods such as molecular dynamic (MD) simulation [1] and continuum theories. MD simulation demands complicated and lengthy calculations; therefore, it is not economical. Recently, higher-order continuum theories, due to their capabilities in the nanoscale, have attracted considerable attention.

In view of the extensive application of SWCNTs, their mechanical modeling is of considerable significance. Since SWCNTs are geometrically similar to cylindrical shells, they could be modeled by cylindrical shells. Hence, in this paper, because of the practicality of vibration and torsional static analysis, the nano-shell formulation was developed. Besides, due to the examination of nano-shells in nano-dimensions, use of higher-order continuum theories and consideration of size effects can predict the dynamic behavior of such nano-structures. These theories include couple stress theory [2–11], modified strain gradient theory [12–20] and surface stress theory [21–23].

In recent years, special attention has been drawn to the use of modified strain gradient theory and couple stress theory in investigation of the mechanical behavior of micro-/nano-structures. Akgöz et al. examined microbeam buckling using strain gradient theory and modified couple stress theory. They used the Euler–Bernoulli model to examine buckling for the size parameter in various boundary conditions [24]. Wang et al. examined the free vibration and static bending of Timoshenko beam using strain gradient theory. They examined size effects and Poisson's coefficient on natural frequency and beam deformation, demonstrating that the size parameter has a considerable impact on natural frequency [25]. Zhao et al. examined nonlinear vibration, buckling and static

✉ Hamid Zeighampour  
h.zeighampour@yahoo.com

Yaghoub Tadi Beni  
tadi@eng.aku.ac.ir

<sup>1</sup> Faculty of Engineering, Shahrekord University, Shahrekord, Iran

bending of the Euler–Bernoulli beam with distributed load using strain gradient theory. They compared frequency, critical load and deformation of the beam with the linear case and the classical theory [26]. Yin et al. examined the free vibration of fluid-conveying microbeam, demonstrating that increase in fluid velocity is accompanied by decrease in natural frequencies, and compared to couple stress theory and the classical theory, strain gradient theory predicts natural frequencies with higher values [27].

In recent year, vibration and torsional instability of micro-/nano- structures have drawn researchers' attention. Natsuki et al. examined instability of the double-walled SWCNT using the classical theory and the shell model. They calculated the critical torsional force resulting from the torsional buckling of the double-walled nanotube for values of different parameters [28]. Asghari et al. [29] modeled the torsional instability of nano-peapod using the non-local theory and the shell model and examined the critical torsional buckling for different parameters. Gheshlaghi et al. [30] studied microbeam torsional vibration using couple stress theory, demonstrating that increase in the size parameter accompanies increase in SWCNT vibrational frequency. Lim et al. [31] examined the torsional vibration of a SWCNT using the non-local theory. They examined the effect of size parameter and boundary conditions on SWCNT frequencies. They also examined SWCNT torsional vibration with longitudinal motion.

Considering the above discussion, in this paper, torsional equations of motion of the cylindrical shell are developed using modified strain gradient theory. Development of these equations is aimed at achieving two basic objectives overlooked by previous research. These objectives are as follows.

First, because of the use of modified strain gradient theory, the newly developed formulation is able to model size effects; therefore, it is appealing and has extensive application in nanoscale modeling. Hence, torsional vibration and static analysis of nanoscale structures can be examined using this formulation.

Second, due the increasing use of elements in the shape of cylindrical shells, such as SWCNTs, in the nanoscale, it is essential to model such elements more precisely. Using the cylindrical shell model instead of the beam model, the new formulation is able to carry out more precise and real simulation of geometrical shapes, and hence, it is appropriate for use in the nanoscale.

After deriving the equations, torsional vibration and static analysis of a SWCNT are examined. For this purpose, the shell theory, taking into consideration the size effect parameter and two types of supports (clamped-free and clamped–clamped), is used. Equations governing the problem as well as boundary conditions derived using Hamilton's principle are discretized through differential quadrature method and are solved under different boundary conditions.

Finally, the effect of various parameters such as size effect and length scale on SWCNT vibration and torsion is examined.

## 2 Preliminaries

### 2.1 Modified Strain Gradient Theory

Modified strain gradient theory contains a new set of equilibrium equations as well as classical equilibrium equations along with five elastic constants. Strain energy for the elastic and isotropic substance in area  $\Lambda$  (with volume element  $V$ ) with infinitesimal deformation is obtained as [32]:

$$U = \frac{1}{2} \int_{\Omega} (\sigma_{ij} \varepsilon_{ij} + p_i \gamma_j + \tau_{ijk}^{(1)} \eta_{ijk}^{(1)} + m_{ij}^s \chi_{ij}^s) dV \quad (1)$$

where  $\varepsilon_{ij}$  is the strain tensor,  $\gamma_j$  is the dilatation gradient vector,  $\eta_{ijk}^{(1)}$  is the deviatoric stretch gradient tensor,  $\chi_{ij}^s$  is the symmetric rotation gradient tensor, which are defined by

$$\varepsilon_{ij} = \frac{1}{2} (\partial_i u_j + \partial_j u_i) \quad (2)$$

$$\gamma_i = \eta_{imm} \quad (3)$$

$$\eta_{ijk}^{(1)} = \eta_{ijk}^s - \frac{1}{5} (\delta_{ij} \eta_{ppk}^s + \delta_{ik} \eta_{ppj}^s + \delta_{jk} \eta_{ppi}^s),$$

$$\eta_{ijk}^s = \frac{1}{3} (\eta_{ijk} + \eta_{jki} + \eta_{kij}), \quad (4)$$

$$\chi_{ij}^s = \frac{1}{4} (e_{ipq} \eta_{jppq} + e_{jppq} \eta_{ipq}) \quad (5)$$

where  $u_i$ ,  $\delta_{ij}$  and  $e_{jppq}$  are the displacement vector components, the Kronecker delta and permutation symbol, respectively. Also,  $\sigma_{ij}$ ,  $p_i$ ,  $\tau_{ijk}^{(1)}$ ,  $m_{ij}^s$ , respectively, stand for the components of Cauchy tensor and higher-order tensors, which are defined using constitutive equations in strain gradient theory in the elastic area as:

$$\sigma_{ij} = C_{ijkl} \varepsilon_{kl} \quad (6)$$

$$p_i = 2l_0^2 \mu \gamma_j \quad (7)$$

$$\tau_{ijk}^{(1)} = 2l_1^2 \mu \eta_{ijk}^{(1)} \quad (8)$$

$$m_{ij}^s = 2l_2^2 \mu \chi_{ij}^s \quad (9)$$

In the above equation,  $\mu$ ,  $C_{ijkl}$  represent shear modulus and elastic constants, respectively;  $l_0$ ,  $l_1$  and  $l_2$  represent extra length parameters dependent on dilatation gradient, deviatoric stretch gradient and symmetric rotation gradient, respectively.

### 2.2 Classical and Higher-Order Strains in the Cylindrical Shell

In general, classical and higher-order strains in cylindrical coordinates and shell theory are obtained as [33]:

$$\begin{aligned}
 \varepsilon_{zz} &= \frac{\partial w}{\partial z}, \quad \varepsilon_{\theta\theta} = \frac{1}{R(1+z/R)} \left[ \frac{\partial v}{\partial \theta} + w \right], \quad \varepsilon_{xx} = \frac{\partial u}{\partial x} \quad (10) \\
 \varepsilon_{\theta z} = \varepsilon_{z\theta} &= \frac{1}{2} \left[ \frac{1}{R(1+z/R)} \frac{\partial w}{\partial \theta} + \frac{\partial v}{\partial z} - \frac{v}{R(1+z/R)} \right], \\
 \varepsilon_{zx} = \varepsilon_{xz} &= \frac{1}{2} \left[ \frac{\partial w}{\partial x} + \frac{\partial u}{\partial z} \right], \\
 \varepsilon_{x\theta} = \varepsilon_{\theta x} &= \frac{1}{2} \left[ \frac{\partial v}{\partial x} + \frac{1}{R(1+z/R)} \frac{\partial u}{\partial \theta} \right], \\
 \eta_{xxx} &= \frac{\partial^2 u}{\partial x^2}, \quad \eta_{xx\theta} = \frac{\partial^2 v}{\partial x^2}, \\
 \eta_{x\theta\theta} = \eta_{\theta x\theta} &= \frac{1}{R(1+z/R)} \left[ \frac{\partial^2 v}{\partial x \partial \theta} + \frac{\partial w}{\partial x} \right], \\
 \eta_{\theta xx} = \eta_{x\theta x} &= \frac{1}{R(1+z/R)} \frac{\partial^2 u}{\partial x \partial \theta}, \\
 \eta_{\theta\theta x} &= \frac{1}{R(1+z/R)} \left[ \frac{1}{R(1+z/R)} \frac{\partial^2 u}{\partial \theta^2} + \frac{\partial u}{\partial z} \right], \\
 \eta_{\theta\theta\theta} &= \frac{1}{[R(1+z/R)]^2} \left[ \frac{\partial^2 v}{\partial \theta^2} + 2 \frac{\partial w}{\partial \theta} \right. \\
 &\quad \left. + R(1+z/R) \frac{\partial v}{\partial z} - v \right], \\
 \eta_{\theta\theta z} &= \frac{1}{[R(1+z/R)]^2} \left[ \frac{\partial^2 w}{\partial \theta^2} - 2 \frac{\partial v}{\partial \theta} \right. \\
 &\quad \left. + R(1+z/R) \frac{\partial w}{\partial z} - w \right], \\
 \eta_{z\theta\theta} = \eta_{\theta z\theta} &= \frac{1}{R(1+z/R)} \left[ \frac{\partial^2 v}{\partial z \partial \theta} - \frac{1}{R(1+z/R)} \frac{\partial v}{\partial \theta} \right. \\
 &\quad \left. + \frac{\partial w}{\partial z} - \frac{w}{R(1+z/R)} \right], \\
 \eta_{zz\theta} &= \frac{\partial^2 v}{\partial z^2}, \quad \eta_{z\theta z} = \eta_{\theta z z} = \frac{1}{R(1+z/R)} \\
 &\quad \times \left[ \frac{\partial^2 w}{\partial z \partial \theta} - \frac{1}{R(1+z/R)} \frac{\partial w}{\partial \theta} - \frac{\partial v}{\partial z} + \frac{v}{R(1+z/R)} \right], \\
 \eta_{xxz} &= \frac{\partial^2 w}{\partial x^2}, \quad \eta_{zxx} = \eta_{xzx} = \frac{\partial^2 u}{\partial x \partial z}, \\
 \eta_{zzz} &= \frac{\partial^2 w}{\partial z^2}, \quad \eta_{z z z} = \frac{\partial^2 u}{\partial z^2}, \quad \eta_{z x z} = \eta_{x z z} = \frac{\partial^2 w}{\partial x \partial z}, \\
 \eta_{z\theta x} = \eta_{\theta z x} &= \frac{1}{R(1+z/R)} \left[ \frac{\partial^2 u}{\partial z \partial \theta} - \frac{1}{R(1+z/R)} \frac{\partial u}{\partial \theta} \right], \\
 \eta_{zx\theta} = \eta_{x z \theta} &= \frac{\partial^2 v}{\partial x \partial z}, \\
 \eta_{x\theta z} = \eta_{\theta x z} &= \frac{1}{R(1+z/R)} \left[ \frac{\partial^2 w}{\partial x \partial \theta} - \frac{\partial v}{\partial x} \right].
 \end{aligned}
 \tag{11}$$

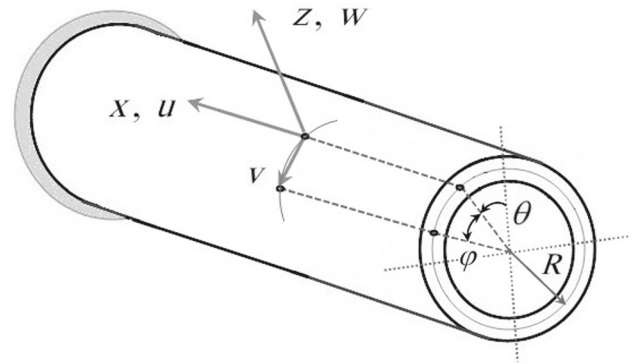


Fig. 1 SWCNT with clamped-free support

### 2.3 Equations of Motion and Corresponding Boundary Conditions

Figure 1 illustrates the nano-shell with clamped-free support where  $R$  is the SWCNT diameter.

Based on the shell model, and with the assumption that the shell is only under torsional vibration and hence its cross section will not undergo elastic deformation, displacement is expressed as [34]:

$$\begin{aligned}
 u(x, \theta, z, t) &= 0, \\
 v(x, \theta, z, t) &= (R+z) \varphi(x, t) \\
 w(x, \theta, z, t) &= 0.
 \end{aligned}
 \tag{12}$$

where  $u, v$  and  $w$  are displacement vectors along  $x, \theta$  and  $z$  axes, respectively, and  $t$  stands for time. As illustrated by Fig. 1, rotation vector  $\varphi$  is expressed around  $x$ -axis.

Besides, classical and high-order strains are calculated by considering the assumption of Love’s thin shell theory ( $(1+z/R) \approx 1$ ). By substituting Eq. (12) into Eqs. (10) and (11), classical and higher-order strains are obtained as:

$$\begin{aligned}
 \varepsilon_{xx} = \varepsilon_{\theta\theta} = \varepsilon_{zz} = \varepsilon_{z\theta} = \varepsilon_{zx} &= 0, \quad \varepsilon_{x\theta} = \frac{R}{2} \left( \frac{\partial \varphi}{\partial x} \right), \\
 \eta_{xx\theta} = R \frac{\partial^2 \varphi}{\partial x^2}, \quad \eta_{x\theta z} = \eta_{\theta x z} &= - \left( \frac{\partial \varphi}{\partial x} \right), \\
 \eta_{xxx} = \eta_{x\theta\theta} = \eta_{\theta x\theta} = \eta_{\theta xx} = \eta_{x\theta x} &= \eta_{\theta\theta x} = \eta_{\theta\theta z} = 0, \\
 \eta_{\theta\theta\theta} = \eta_{z\theta\theta} = \eta_{\theta z\theta} = \eta_{xxz} = \eta_{zxx} &= \eta_{xzx} = \eta_{zx\theta} \\
 &= \eta_{x z \theta} = 0, \\
 \eta_{zzz} = \eta_{z\theta z} = \eta_{\theta z z} = \eta_{z\theta x} = \eta_{\theta z x} &= \eta_{z z x} = \eta_{z x z} \\
 &= \eta_{x z z} = \eta_{z z \theta} = 0.
 \end{aligned}
 \tag{14}$$

By substituting Eq. (14) into Eq. (5), symmetric rotation gradient strains are obtained as:

$$\chi_{zz} = \chi_{\theta x} = \chi_{x\theta} = \chi_{\theta z} = \chi_{z\theta} = 0,$$

$$\begin{aligned}\chi_{xx} &= -\frac{1}{2} \left( \frac{\partial \varphi}{\partial x} \right), \quad \chi_{\theta\theta} = \frac{1}{2} \left( \frac{\partial \varphi}{\partial x} \right), \\ \chi_{xz} &= \chi_{zx} = \frac{R}{4} \left( \frac{\partial^2 \varphi}{\partial x^2} \right).\end{aligned}\quad (15)$$

By substituting Eq. (14) into Eq. (4), deviatoric stretch gradient strains are expressed as:

$$\begin{aligned}\eta_{\theta\theta x}^{(1)} &= \eta_{x\theta\theta}^{(1)} = \eta_{\theta x\theta}^{(1)} = \eta_{\theta\theta z}^{(1)} = \eta_{z\theta\theta}^{(1)} = \eta_{\theta z\theta}^{(1)} = 0, \\ \eta_{xxz}^{(1)} &= \eta_{zxx}^{(1)} = \eta_{xzx}^{(1)} = \eta_{z zx}^{(1)} = \eta_{zxz}^{(1)} = \eta_{xzz}^{(1)} \\ &= \eta_{xxx}^{(1)} = \eta_{zzz}^{(1)} = 0, \\ \eta_{zz\theta}^{(1)} &= \eta_{\theta zz}^{(1)} = \eta_{z\theta z}^{(1)} = -\frac{R}{15} \left( \frac{\partial^2 \varphi}{\partial x^2} \right), \\ \eta_{xx\theta}^{(1)} &= \eta_{\theta xx}^{(1)} = \eta_{x\theta x}^{(1)} = \frac{4R}{15} \left( \frac{\partial^2 \varphi}{\partial x^2} \right), \\ \eta_{\theta\theta\theta}^{(1)} &= -\frac{R}{5} \left( \frac{\partial^2 \varphi}{\partial x^2} \right), \quad \eta_{x\theta z}^{(1)} = \eta_{\theta xz}^{(1)} = \eta_{zx\theta}^{(1)} = \eta_{xz\theta}^{(1)} \\ &= \eta_{z\theta x}^{(1)} = \eta_{\theta zx}^{(1)} = -\frac{1}{3} \left( \frac{\partial \varphi}{\partial x} \right).\end{aligned}\quad (16)$$

By substituting Eq. (14) into Eq. (3), dilatation gradient strains are expressed as:

$$\gamma_x = \gamma_\theta = \gamma_z = 0, \quad (17)$$

The nonzero stresses  $\sigma$  are obtained by substituting Eq. (13) into Eq. (6) as follows:

$$\sigma_{x\theta} = \mu R \left( \frac{\partial \varphi}{\partial x} \right). \quad (18)$$

By substituting Eq. (15) into Eq. (9), the components of non-classical stresses  $\chi$  are obtained as follows:

$$\begin{aligned}m_{xx} &= -\mu l_2^2 \left( \frac{\partial \varphi}{\partial x} \right), \quad m_{\theta\theta} = \mu l_2^2 \left( \frac{\partial \varphi}{\partial x} \right), \quad m_{xz} = m_{zx} \\ &= \frac{\mu l_2^2 R}{2} \left( \frac{\partial^2 \varphi}{\partial x^2} \right).\end{aligned}\quad (19)$$

By substituting Eq. (16) into Eq. (8), the components of non-classical stresses  $\eta$  are obtained as follows:

$$\begin{aligned}\tau_{zz\theta}^{(1)} &= \tau_{\theta zz}^{(1)} = \tau_{z\theta z}^{(1)} = -\frac{2\mu l_1^2 R}{15} \left( \frac{\partial^2 \varphi}{\partial x^2} \right), \\ \tau_{xx\theta}^{(1)} &= \tau_{\theta xx}^{(1)} = \tau_{x\theta x}^{(1)} = \frac{8\mu l_1^2 R}{15} \left( \frac{\partial^2 \varphi}{\partial x^2} \right), \\ \tau_{\theta\theta\theta}^{(1)} &= -\frac{2\mu l_1^2 R}{5} \left( \frac{\partial^2 \varphi}{\partial x^2} \right), \quad \tau_{x\theta z}^{(1)} = \tau_{\theta xz}^{(1)} = \tau_{zx\theta}^{(1)} = \tau_{xz\theta}^{(1)} \\ &= \tau_{z\theta x}^{(1)} = \tau_{\theta zx}^{(1)} = -\frac{2\mu l_1^2}{3} \left( \frac{\partial \varphi}{\partial x} \right).\end{aligned}\quad (20)$$

In this paper, Hamilton's principle was used to derive the equations. As is clear, to use Hamilton's principle, it is necessary to calculate strain energy, kinetic energy and the work done by external loads acting on the shell. In Eqs. (13)–(17), strains are calculated in the strain gradient theory and the shell model. Now, by substituting these equations in the constitutive equations in (6)–(9), one can calculate the components of classical and non-classical stress tensor. And by substituting the result for the components of classical and non-classical stress and strain in Eq. (1) and simplifying it, strain energy is obtained as follows:

$$\begin{aligned}U_s &= \frac{1}{2} \int_0^{2\pi} \int_0^L \left\{ \left[ N_{x\theta} - \frac{Y_{xx}^{(2)}}{2R} + \frac{Y_{\theta\theta}^{(2)}}{2R} - \frac{2Y_{\theta xz}^{(1)}}{R} \right] \frac{\partial \varphi}{\partial x} \right. \\ &\quad \left. + \left[ \frac{Y_{zx}^{(2)}}{2} - \frac{Y_{\theta\theta\theta}^{(1)}}{5} - \frac{Y_{z\theta z}^{(1)}}{5} + \frac{4Y_{x\theta x}^{(1)}}{5} \right] \frac{\partial^2 \varphi}{\partial x^2} \right\} R^2 dx d\theta\end{aligned}\quad (21)$$

In the above equations, classical and higher-order forces and moments are written as follows:

$$N_{ij} = \int_{-h/2}^{h/2} \sigma_{ij} dz, \quad (22)$$

$$Y_{ij}^{(2)} = \int_{-h/2}^{h/2} m_{ij} dz, \quad (23)$$

$$Y_{ijk}^{(1)} = \int_{-h/2}^{h/2} \tau_{ijk}^{(1)} dz, \quad (24)$$

The kinetic energy for nano-shell is stated as follows:

$$T = \frac{1}{2} \rho \int_A \int_{-h/2}^{h/2} R^2 \left( \frac{\partial \varphi}{\partial t} \right)^2 dz dA \quad (25)$$

where  $\rho$  is the material density.

The work of external load acting on the nano-shell is expressed as:

$$W = \int_0^L T(x, t) \varphi dx + \bar{T} \varphi \Big|_{x=0, L}^+ \bar{T}^h \left( \frac{\partial \varphi}{\partial x} \right) \Big|_{x=0, L} \quad (26)$$

By using Hamilton's principle ( $\int_{t_1}^{t_2} (\delta T - \delta U + \delta W) dt = 0$ ) and substituting Eqs. (21)–(26) into it, performing variation and integration by parts, discretizing the equations, and performing some mathematical calculations, the equation of motion and boundary conditions is obtained as follows:

$$S_1 \frac{\partial^4 \varphi}{\partial x^4} - S_2 \frac{\partial^2 \varphi}{\partial x^2} + \rho h \frac{\partial^2 \varphi}{\partial t^2} = T(x, t), \quad (27)$$

where

$$S_1 = \mu h \left( \frac{8l_1^2}{15} + \frac{l_2^2}{4} \right), \quad S_2 = \mu h \left( 1 + \frac{4l_1^2}{3R^2} + \frac{l_2^2}{R^2} \right), \quad (28)$$

And boundary conditions will be as follows:

$$\left\{ \begin{aligned} & \frac{\partial \varphi}{\partial x} \left[ \mu h \left( 1 + \frac{4l_1^2}{3R^2} + \frac{l_2^2}{R^2} \right) \right] \\ & - \frac{\partial^3 \varphi}{\partial x^3} \left[ \mu h \left( \frac{8l_1^2}{15} + \frac{l_2^2}{4} \right) \right] - \bar{T} \end{aligned} \right\} \Big|_{x=0,L} = 0 \quad \text{or} \\ \delta \varphi|_{x=0,L} = 0 \\ \left\{ \begin{aligned} & \frac{\partial^2 \varphi}{\partial x^2} \left[ \mu h \left( \frac{8l_1^2}{15} + \frac{l_2^2}{4} \right) \right] - \bar{T}^h \end{aligned} \right\} \Big|_{x=0,L} = 0 \quad \text{or} \\ \delta \left( \frac{\partial \varphi}{\partial x} \right) \Big|_{x=0,L} = 0 \end{aligned} \quad (29)$$

Equations (27) and (29) are equations of torsional motion and classical and non-classical boundary conditions for the cylindrical shell in the strain gradient theory which is reduced to the following theories in the special case:

If the size parameters are assumed as  $l_0 = l_1 = 0$  and  $l_2 = l$  in the equations derived, the governing equations in strain gradient theory are reduced to modified couple stress theory.

If the size parameters are assumed as  $l_0 = l_1 = l_2 = 0$  in the equations derived, the governing equations in the modified couple stress theory are reduced to the classical continuum theory [34].

### 3 Examination of the Vibration and Static Torsional Behavior of the SWCNT as the Special Application of the Formulation Developed

#### 3.1 Free Vibration Case

Using the equation of motion and boundary conditions in Eqs. (27) and (29), free torsional vibration equation for a SWCNT with length  $L$ , radius  $R$  and thickness  $h$ , in clamped-free and clamped–clamped support conditions, is expressed as follows:

$$S_1 \frac{\partial^4 \varphi}{\partial x^4} - S_2 \frac{\partial^2 \varphi}{\partial x^2} + \rho h \frac{\partial^2 \varphi}{\partial t^2} = 0, \quad (30)$$

The boundary conditions for the SWCNT with clamped-free support are as follows. In boundary conditions, it is assumed that there is no higher-order force.

$$\varphi(0, t) = 0, \quad \frac{\partial^2 \varphi(0, t)}{\partial x^2} = 0.$$

$$\begin{aligned} & \mu h \left( 1 + \frac{4l_1^2}{3R^2} + \frac{l_2^2}{R^2} \right) \frac{\partial \varphi(L, t)}{\partial x} \\ & - \mu h \left( \frac{8l_1^2}{15} + \frac{l_2^2}{4} \right) \frac{\partial^3 \varphi(L, t)}{\partial x^3} = 0, \\ & \frac{\partial^2 \varphi(L, t)}{\partial x^2} = 0. \end{aligned} \quad (31)$$

And the boundary conditions for the SWCNT with clamped–clamped support are as follows:

$$\begin{aligned} \varphi(0, t) = 0, \quad \frac{\partial^2 \varphi(0, t)}{\partial x^2} = 0. \\ \varphi(L, t) = 0, \quad \frac{\partial^2 \varphi(L, t)}{\partial x^2} = 0. \end{aligned} \quad (32)$$

To solve the vibration problem in Eq. (30) and boundary conditions in Eqs. (31) and (32), the differential quadrature method (DQM) is used. In this method, the derivative of a function at a given point could be stated as a weighted linear summation of the values of the function at all the points in the domain. The  $k$ th derivative of function  $\varphi$  is approximated as [35]:

$$\frac{\partial^k}{\partial \zeta^k} \{ \varphi \} |_{\zeta=\zeta_j} = \sum_{m=1}^N C_{jm}^{(k)} \{ \varphi(\zeta_m, t) \} \quad (33)$$

where  $N$  is the number of nodes in the domain and  $C_{jm}^{(k)}$  is the weighted coefficients obtained through recursive equations. The coefficients of the  $m$ th point are obtained through Chebyshev–Gauss–Lobatto formula [36].

$$\zeta_m = \frac{1}{2} \left[ 1 - \cos \left( \frac{m-1}{N-1} \pi \right) \right], \quad m = 1, 2, \dots, N \quad (34)$$

Equation (26) with one of the boundary conditions in Eqs. (29) and (30) is expressed in the matrix form as:

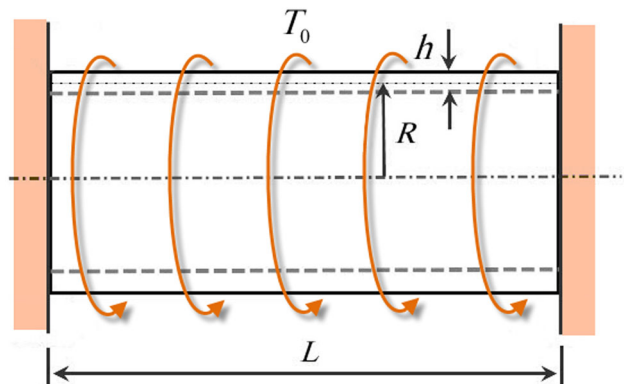


**Fig. 2** SWCNT with clamped–clamped support under distributed torsional load ( $T_0$ )

$$\begin{bmatrix} K_{dd} & K_{db} \\ K_{bd} & K_{bb} \end{bmatrix} \begin{Bmatrix} d_d \\ d_b \end{Bmatrix} + \begin{bmatrix} M_{dd} & M_{db} \\ 0 & 0 \end{bmatrix} \begin{Bmatrix} \ddot{d}_d \\ \ddot{d}_b \end{Bmatrix} = 0 \quad (35)$$

where subscripts d and b are related to the equation of motion and boundary conditions, respectively. The equations are solved using the following equation:

$$\{d_d, d_b\} = \{\bar{d}_d, \bar{d}_b\} e^{\omega t} \quad (36)$$

where  $\omega$  represents the natural frequency. By substituting Eq. (36) in Eq. (35), the results are rewritten as follows:

$$(K + \omega^2 M) \begin{Bmatrix} \tilde{d}_d \\ \tilde{d}_b \end{Bmatrix} = 0 \quad (37)$$

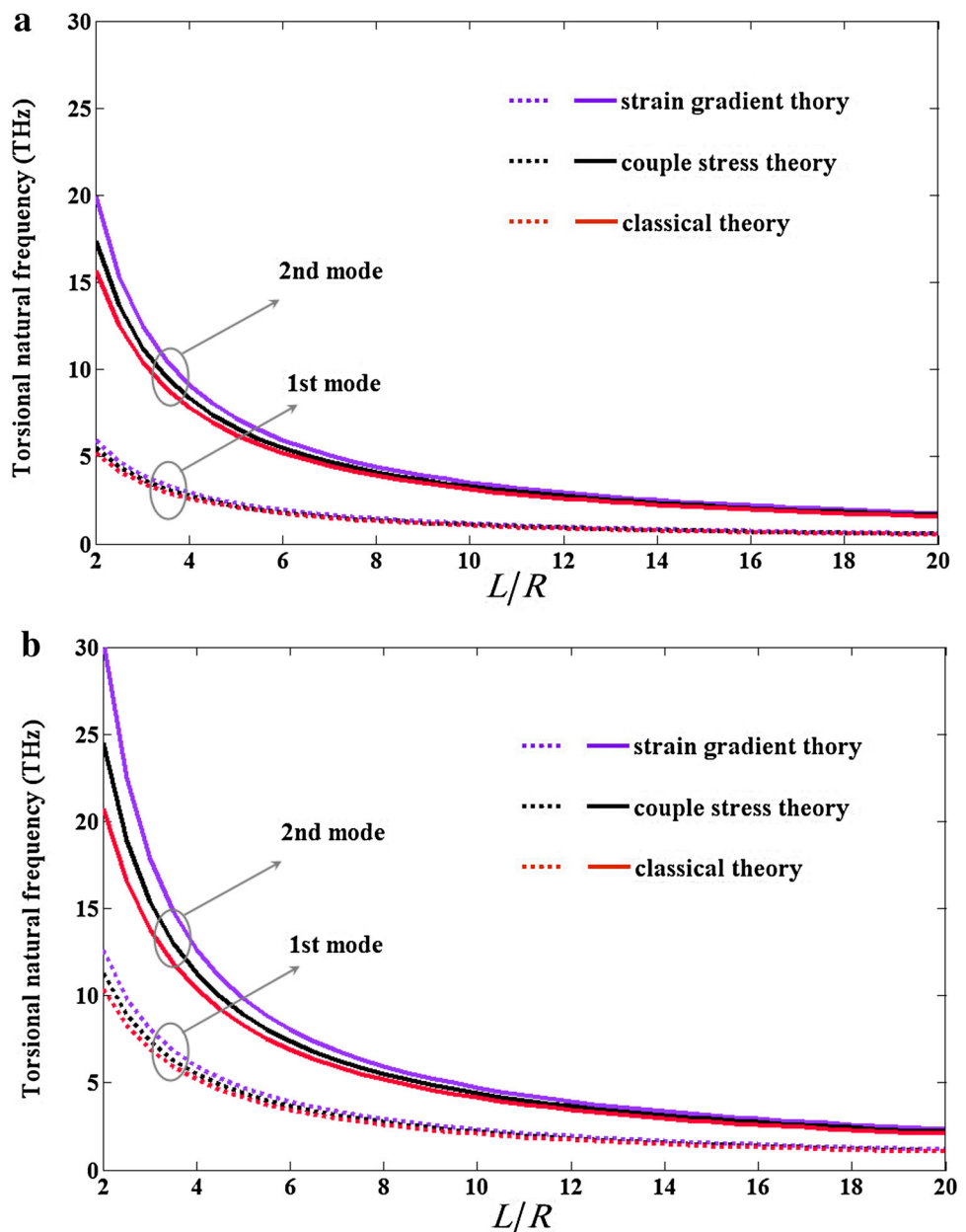
where  $[K]$ ,  $[M]$  are stiffness matrix and mass matrix, respectively, and the natural frequency is obtained from Eq. (37) by setting the determinant of equal coefficients to zero.

### 3.2 Static Case

In this section, for the static case as a case study, a SWCNT under distributed torsional load ( $T_0$ ) with clamped–clamped support is examined as illustrated in Fig. 2.

Using Eq. (27) and clamped–clamped boundary conditions for static torsion case, and considering  $\frac{\partial}{\partial t} = 0$  and  $\frac{\partial \varphi}{\partial x} = \frac{d\varphi}{dx}$ , one can conclude that:

**Fig. 3** SWCNT natural frequency in length–radius ratio and different theories. **a** Clamped–free support, **b** clamped–clamped support



$$S_1 \frac{d^4 \varphi}{dx^4} - S_2 \frac{d^2 \varphi}{dx^2} = T_0, \tag{38}$$

$$\varphi(0, t) = 0, \frac{d^2 \varphi(0, t)}{dx^2} = 0. \quad \varphi(L, t) = 0, \frac{d^2 \varphi(L, t)}{dx^2} = 0. \tag{39}$$

where

$$\lambda_1 = \sqrt{\frac{S_2}{S_1}} \tag{41}$$

Equation (38) is a non-homogeneous linear ordinary differential equation with constant coefficients, which can be analytically solved. The solution to the above differential equation, which includes general and special solutions, is expressed as:

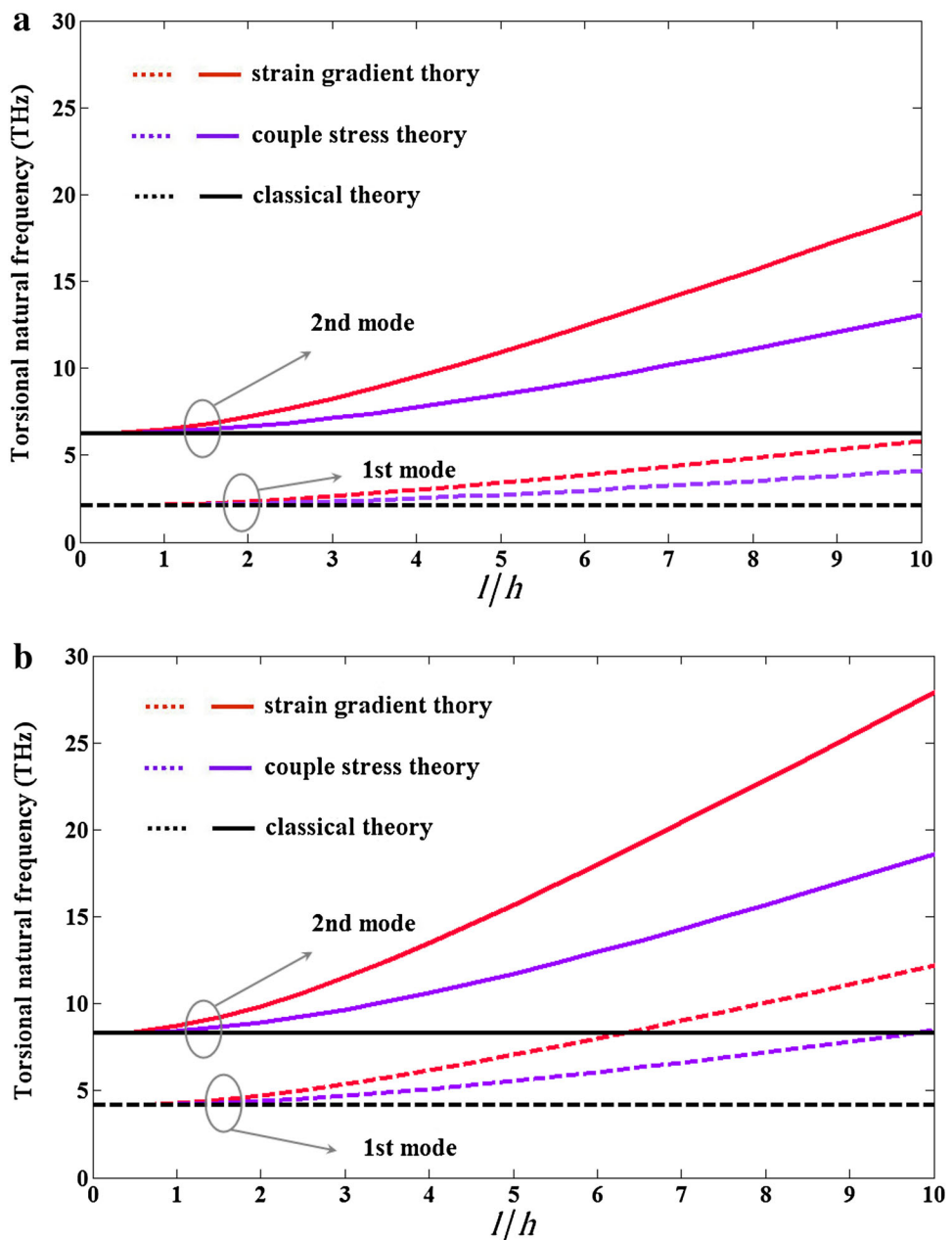
$$\varphi(x) = C_1 + C_2 x + C_3 e^{-\lambda_1 x} + C_4 e^{\lambda_1 x} - \frac{T_0}{2S_2} x^2 \tag{40}$$

Equation (40) is the analytical solution for SWCNT static torsion obtained using modified strain gradient theory. In this equation, constant coefficients  $C_1$  and  $C_4$  are calculated using boundary conditions in Eq. (39), which are as follows

$$C_1 = -T_0/\lambda_1^2 S_2 \tag{42}$$

$$C_2 = T_0 L/2S_2 \tag{43}$$

**Fig. 4** SWCNT natural frequency in size parameter and different theories. **a** Clamped-free support, **b** clamped-clamped support



$$C_3 = T_0 \left( e^{\lambda_1 L} - 1 \right) / \lambda_1^2 S_2 \left( e^{2\lambda_1 L} - 1 \right) \quad (44)$$

$$C_4 = T_0 \left( e^{2\lambda_1 L} - e^{\lambda_1 L} \right) / \lambda_1^2 S_2 \left( e^{2\lambda_1 L} - 1 \right) \quad (45)$$

## 4 Discussion and Conclusions for SWCNT Torsion

### 4.1 Free Vibration of SWCNT

In this section, the free vibration of the SWCNT is examined using the shell theory. Boundary conditions are considered as clamped–clamped and clamped–free. The effects of various parameters such as size effect and length–radius ratio are determined using modified strain gradient theory and are compared with the couple stress theory and classical theory. Geometrical and mechanical characteristics for solving the problem of SWCNT vibration are as follows:

$$R = 2 \text{ nm}, \quad h = 0.34 \text{ nm}, \quad E = 1 \text{ GPa}, \quad L = 10 \text{ nm}, \\ \nu = 0.25, \quad \rho_t = 2300 \text{ kg/m}^3. \quad (46)$$

Incidentally, in this section, to better express the results, size parameters are assumed as  $l = l_2 = l_1 = l_0$ .

Figure 3 displays the effect of length–radius ratio on the natural frequency of SWCNT with clamped–free and clamped–clamped supports for the two first frequency modes and for  $l/h = 2$ . As illustrated, increase in length–radius ratio is accompanied by decrease in SWCNT natural frequency, which is due to reduction in SWCNT rigidity in bigger length–diameter ratios. In strain gradient theory and couple stress theory, increase in length–diameter ratio is accompanied by decrease in the effect of size parameter on SWCNT natural frequency and nears the values of frequencies of the classical theory. Consequently, in shorter lengths, the size parameter in higher-order theories has greater effect on natural frequencies. The values of frequencies obtained in clamped–clamped supported SWCNT are greater than in clamped–free supported SWCNT. This is due to the greater rigidity of the SWCNT with clamped–clamped support. It can be concluded from Fig. 3 that variation of natural frequency in the second mode is more than that in the first mode.

Figure 4 illustrates the natural frequency of the SWCNT for different size parameters. Increase in the size parameter is accompanied by increase in SWCNT natural frequency. This is due to the increase in SWCNT rigidity. Increase in natural frequency in the strain gradient theory is greater than that in the couple stress theory and the classical theory, which is due to the presence of three size parameters in strain gradient theory and one size parameter in couple stress theory. Variation of frequency in the clamped–clamped supported SWCNT is

higher than that in the clamped–free supported SWCNT and the second mode.

### 4.2 Torsional Static Analysis of SWCNT

In this section, the effect of size parameter and length variation on torsional static analysis of the SWCNT is examined. Figure 5 illustrates the ratio of SWCNT torsion angle to the thickness in various size parameters on the basis of SWCNT length. In this case,  $L/R = 5$  and the support is clamped–clamped. It can be concluded from the illustration that increase in size effect, i.e., increase in the  $l/h$  ratio, is accompanied by decrease in SWCNT torsion angle. In fact, increase in the size parameter is accompanied by increase in SWCNT rigidity. Consequently, as rigidity increases, the torsion angle of the SWCNT decreases. On the other hand, as illustrated by Fig. 5, as the size parameter changes, the variation in torsion angle across the SWCNT is slighter, and decrease in size parameter renders the variation in torsion angle at the two ends greater.

Figure 6 illustrates the effect of SWCNT length variation on SWCNT torsion in various length–diameter ratios. In this illustration, the size parameter is considered as  $l/h = 1$ ; hence, the solution displayed is dependent on the size effect. As illustrated by Fig. 6, increase in SWCNT length is accompanied by increase in the ratio of torsion angle to thickness. In other words, as SWCNT length increases, the torsion angle of SWCNT increases, too. Figure 6 also shows that as the ratio of length to radius of the SWCNT increases, the variation in torsion angle becomes slighter in the central points and greater at the two ends.

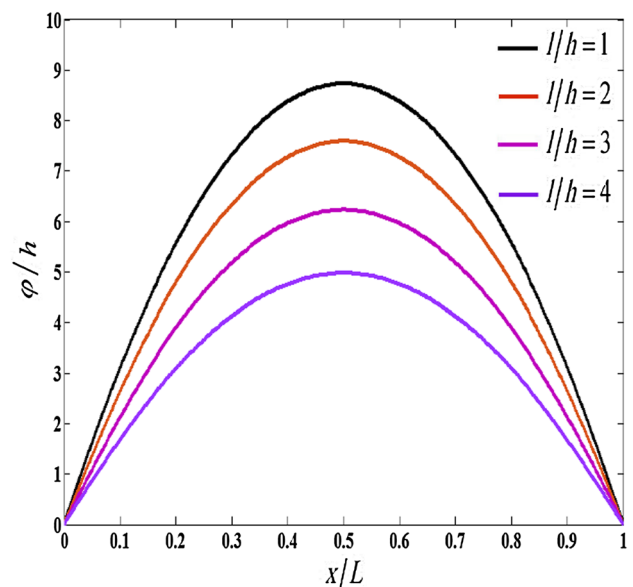


**Fig. 5** Effect of size parameter based on the ratio of torsion angle to thickness



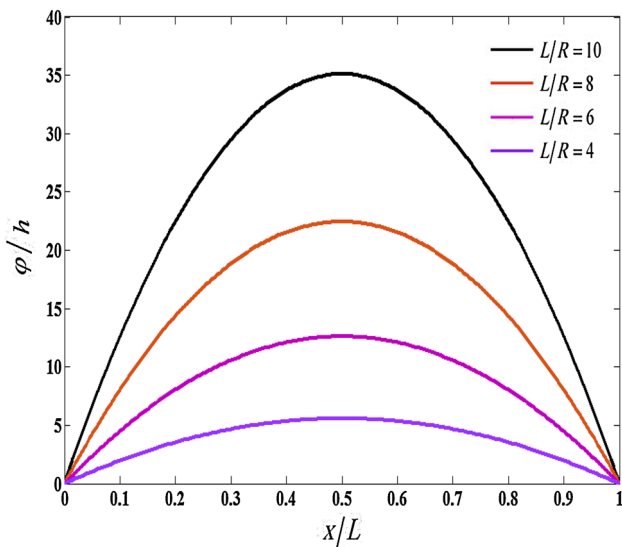


Fig. 6 Effect of length–radius ratio based on the ratio of torsion angle to thickness

### 4.3 Validation of Result

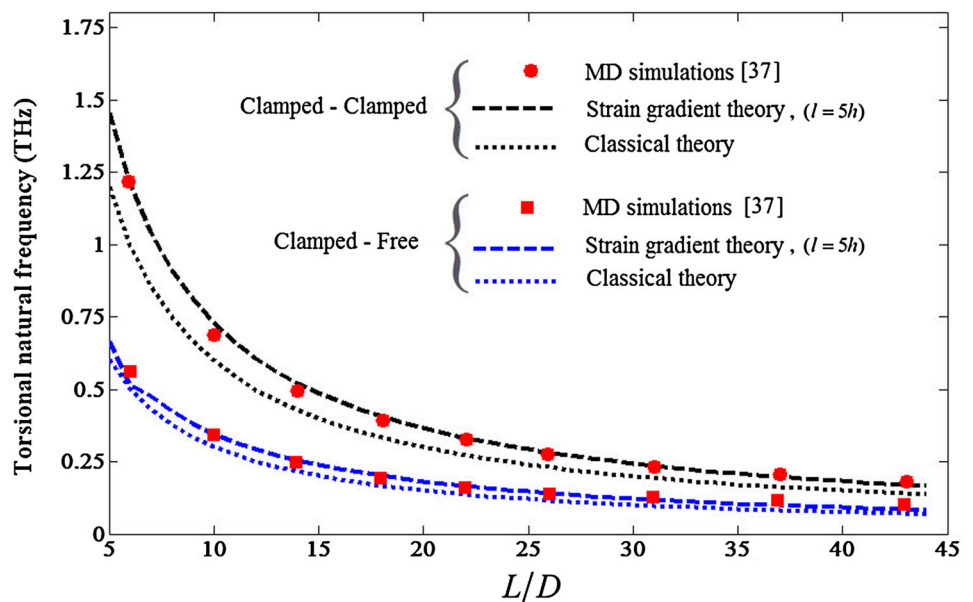
In this section, the results of the torsional vibration frequency of SWCNT obtained with the new model proposed in this article have been compared with the molecular dynamic (MD) simulation [37]. In addition, a comparison is drawn between the results of the two clamped–clamped and clamped-free cases. According to Fig. 7 in the size parameter ( $l = 5h$ ), the torsional vibration frequency of SWCNT using strain gradient theory has good math with MD simulation results. However, despite the classic model, torsional vibration frequency provided by the present size-dependent model is very close to MD simulation values. The value of size parameters

is selected as ( $l = 5h$ ) to produce the best fit with the MD simulation. Interestingly, this model is able to accurately predict the torsional vibration frequency of the SWCNT. It can be concluded that the present size-dependent model might fill the gap between MD simulation results and previous classic theoretical models.

### 5 Conclusion

In this paper, equations of torsional motion of the cylindrical shell were developed by using modified strain gradient theory. The purpose of the development of the equations was to achieve the two basic goals of modeling with more precise geometry and taking into consideration size effects in micro-/nanoscale. To achieve this purpose, by using modified strain gradient theory and Hamilton’s principle, the higher-order equations as well as boundary conditions of the SWCNT were obtained. Afterward, using differential quadrature method, the equations with boundary conditions for the free vibration of a SWCNT were discretized, and the torsional natural frequencies of the eigenvalue problem were determined. The boundary conditions were considered as clamped–clamped and clamped-free supports, and the natural frequencies of the SWCNT for various parameters such as size parameter and length–diameter ratio were examined and were compared to couple stress theory and the classical theory. Results demonstrated that the torsional natural frequencies obtained for the SWCNT using modified strain gradient theory are higher than those obtained using couple stress theory and the classical theory. The natural frequency in the clamped–clamped case is higher than that in the clamped-free case. In the smaller length–diameter ratio, the effect of size parameter on SWCNT natural frequency is

Fig. 7 Comparison of torsional natural frequencies between strain gradient theory and MD simulation for the two cases: clamped–clamped and clamped-free supported SWCNT



greater. Results also reveal that increase in the size parameter and decrease in SWCNT length are accompanied by decrease in SWCNT torsion. In addition, torsional static analysis of the SWCNT with clamped–clamped support is examined, which shows the formulation power in static and dynamic analyses.

## References

- Zhou, L.; Shi, S.: Molecular dynamic simulations on tensile mechanical properties of single-walled carbon nanotubes with and without hydrogen storage. *Comput. Mater. Sci.* **23**(1), 166–174 (2002)
- Wang, L.; Xu, Y.Y.; Ni, Q.: Size-dependent vibration analysis of three-dimensional cylindrical microbeams based on modified couple stress theory: a unified treatment. *Int. J. Eng. Sci.* **68**, 1–10 (2013). doi:10.1016/j.ijengsci.2013.03.004
- Akgöz, B.; Civalek, Ö.: Modeling and analysis of micro-sized plates resting on elastic medium using the modified couple stress theory. *Meccanica* **48**(4), 863–873 (2013)
- Zeighampour, H.; Beni, Y.T.: A shear deformable cylindrical shell model based on couple stress theory. *Arch. Appl. Mech.* **85**(4), 539–553 (2014)
- Zeighampour, H.; Beni, Y.T.: Free vibration analysis of axially functionally graded nanobeam with radius varies along the length based on strain gradient theory. *Appl. Math. Model.* **39**(18), 5354–5369 (2015)
- Zeighampour, H.; Beni, Y.T.: Size-dependent vibration of fluid-conveying double-walled carbon nanotubes using couple stress shell theory. *Phys. E* **61**, 28–39 (2014)
- Dehrouyeh-Semnani, A.M.: The influence of size effect on flapwise vibration of rotating microbeams. *Int. J. Eng. Sci.* **94**, 150–163 (2015)
- Beni, Y.T.; Mehralian, F.; Razavi, H.: Free vibration analysis of size-dependent shear deformable functionally graded cylindrical shell on the basis of modified couple stress theory. *Compos. Struct.* **120**, 65–78 (2015)
- Zeighampour, H.; Beni, Y.T.; Mehralian, F.: A shear deformable conical shell formulation in the framework of couple stress theory. *Acta Mech.* **226**(8), 2607–2629 (2015)
- Baninajaryan, A.; Beni, Y.T.: Theoretical study of the effect of shear deformable shell model, elastic foundation and size dependency on the vibration of protein microtubule. *J. Theor. Biol.* **382**, 111–121 (2015)
- Shojaeian, M.; Beni, Y.T.: Size-dependent electromechanical buckling of functionally graded electrostatic nano-bridges. *Sens. Actuators A Phys.* **232**(1), 49–62 (2015)
- Das, S.L.; Mandal, T.; Gupta, S.S.: Inextensional vibration of zig-zag single-walled carbon nanotubes using nonlocal elasticity theories. *Int. J. Solids Struct.* **50**(18), 2792–2797 (2013). doi:10.1016/j.ijsolstr.2013.04.019
- Kahrobaiyan, M.; Tajalli, S.; Movahhedy, M.; Akbari, J.; Ahmadian, M.: Torsion of strain gradient bars. *Int. J. Eng. Sci.* **49**(9), 856–866 (2011)
- Akgöz, B.; Civalek, Ö.: Longitudinal vibration analysis for micro-bars based on strain gradient elasticity theory. *J. Vib. Control* **20**(4), 606–616 (2014)
- Akgöz, B.; Civalek, Ö.: A new trigonometric beam model for buckling of strain gradient microbeams. *Int. J. Mech. Sci.* **81**, 88–94 (2014)
- Akgöz, B.; Civalek, Ö.: A microstructure-dependent sinusoidal plate model based on the strain gradient elasticity theory. *Acta Mech.* **226**(7), 2277–2294 (2015)
- Sedighi, H.M.; Koochi, A.; Abadyan, M.: Modeling the size dependent static and dynamic pull-in instability of cantilever nanoactuator based on strain gradient theory. *Int. J. Appl. Mech.* **6**(5), 1450055 (2014)
- Narendar, S.; Ravinder, S.; Gopalakrishnan, S.: Strain gradient torsional vibration analysis of micro/nano rods. *Int. J. Nanodimens.* **3**(1), 1–17 (2012)
- Zeiverdejani, M.K.; Beni, Y.T.: The nano scale vibration of protein microtubules based on modified strain gradient theory. *Curr. Appl. Phys.* **13**(8), 1566–1576 (2013). doi:10.1016/j.cap.2013.05.019
- Beni, Y.T.; Karimipour, I.; Abadyan, M.: Modeling the instability of electrostatic nano-bridges and nano-cantilevers using modified strain gradient theory. *Appl. Math. Model.* **39**(9), 2633–2648 (2015)
- Gurtin, M.E.; Weissmüller, J.; Larché, F.: A general theory of curved deformable interfaces in solids at equilibrium. *Philos. Mag. A* **78**(5), 1093–1109 (1998). doi:10.1080/01418619808239977
- Sahmani, S.; Bahrami, M.; Aghdam, M.: Surface stress effects on the postbuckling behavior of geometrically imperfect cylindrical nanoshells subjected to combined axial and radial compressions. *Int. J. Mech. Sci.* **100**, 1–22 (2015)
- Sedighi, H.M.; Daneshmand, F.; Abadyan, M.: Modified model for instability analysis of symmetric FGM double-sided nano-bridge: corrections due to surface layer, finite conductivity and size effect. *Compos. Struct.* **132**, 545–557 (2015)
- Akgöz, B.; Civalek, Ö.: Strain gradient elasticity and modified couple stress models for buckling analysis of axially loaded micro-scaled beams. *Int. J. Eng. Sci.* **49**(11), 1268–1280 (2011). doi:10.1016/j.ijengsci.2010.12.009
- Wang, B.; Zhao, J.; Zhou, S.: A micro scale Timoshenko beam model based on strain gradient elasticity theory. *Eur. J. Mech. A Solids* **29**(4), 591–599 (2010). doi:10.1016/j.euromechsol.2009.12.005
- Zhao, J.; Zhou, S.; Wang, B.; Wang, X.: Nonlinear microbeam model based on strain gradient theory. *Appl. Math. Model.* **36**(6), 2674–2686 (2012). doi:10.1016/j.apm.2011.09.051
- Yin, L.; Qian, Q.; Wang, L.: Strain gradient beam model for dynamics of microscale pipes conveying fluid. *Appl. Math. Model.* **35**(6), 2864–2873 (2011). doi:10.1016/j.apm.2010.11.069
- Natsuki, T.; Tsuchiya, T.; Ni, Q.-Q.; Endo, M.: Torsional elastic instability of double-walled carbon nanotubes. *Carbon* **48**(15), 4362–4368 (2010). doi:10.1016/j.carbon.2010.07.050
- Asghari, M.; Rafati, J.; Naghdabadi, R.: Torsional instability of carbon nano-peapods based on the nonlocal elastic shell theory. *Phys. E* **47**, 316–323 (2013). doi:10.1016/j.physe.2012.06.016
- Gheshlaghi, B.; Hasheminejad, S.M.; Abbasian, S.: Size dependent torsional vibration of nanotubes. *Phys. E* **43**(1), 45–48 (2010). doi:10.1016/j.physe.2010.06.015
- Lim, C.W.; Li, C.; Yu, J.L.: Free torsional vibration of nanotubes based on nonlocal stress theory. *J. Sound Vib.* **331**(12), 2798–2808 (2012). doi:10.1016/j.jsv.2012.01.016
- Lam, D.C.C.; Yang, F.; Chong, A.C.M.; Wang, J.; Tong, P.: Experiments and theory in strain gradient elasticity. *J. Mech. Phys. Solids* **51**(8), 1477–1508 (2003). doi:10.1016/S0022-5096(03)00053-X
- Zeighampour, H.; Beni, Y.T.: Cylindrical thin-shell model based on modified strain gradient theory. *Int. J. Eng. Sci.* **78**, 27–47 (2014)
- Soedel, W.: *Vibrations of Shells and Plates*. 3rd edn. Taylor & Francis, London (2004)
- Shu, C.: *Differential Quadrature and Its Application in Engineering*. Springer, Berlin (2000)
- Zong, Z.; Zhang, Y.: *Advanced Differential Quadrature Methods*. CRC Press, Boca Raton (2009)
- Ansari, R.; Gholami, R.; Achori, S.: Torsional vibration analysis of carbon nanotubes based on the strain gradient theory and molecular dynamic simulations. *J. Vib. Acoust.* **135**(5), 051016 (2013)

